Molecular Cancer Therapeutics

Combinatorial Therapy of Zinc Metallochaperones with Mutant p53 Reactivation and Diminished Copper Binding

Saif Zaman[1], Xin Yu[2,3], Anthony F. Bencivenga[4], Adam R. Blanden[5], Yue Liu[2,3], Tracy Withers[2,3], Bing Na[2,3], Alan J. Blayney[5], John Gilleran[4], David A. Boothman[6,7], Stewart N. Loh[5], S. David Kimball[4,8,9], and Darren R. Carpizo[2,3,9]

Abstract

Chemotherapy and radiation are more effective in wild-type (WT) p53 tumors due to p53 activation. This is one rationale for developing drugs that reactivate mutant p53 to synergize with chemotherapy and radiation. Zinc metallochaperones (ZMC) are a new class of mutant p53 reactivators that restore WT structure and function to zinc-deficient p53 mutants. We hypothesized that the thiosemicarbazone, ZMC1, would synergize with chemotherapy and radiation. Surprisingly, this was not found. We explored the mechanism of this and found the reactive oxygen species (ROS) activity of ZMC1 negates the signal on p53 that is generated with chemotherapy and radiation. We hypothesized that a zinc scaffold generating less ROS would synergize with chemotherapy and radiation. The ROS effect of ZMC1 is generated by its chelation of redox active copper. ZMC1 copper binding (K_{Cu}) studies reveal its affinity for copper is approximately 10^8 greater than Zn^{2+}. We identified an alternative zinc scaffold (nitrilotriacetic acid) and synthesized derivatives to improve cell permeability. These compounds bind zinc in the same range as ZMC1 but bound copper much less avidly (10^6- to 10^7-fold lower) and induced less ROS. These compounds were synergistic with chemotherapy and radiation by inducing p53 signaling events on mutant p53. We explored other combinations with ZMC1 based on its mechanism of action and demonstrate that ZMC1 is synergistic with MDM2 antagonists, BCL2 antagonists, and molecules that deplete cellular reducing agents. We have identified an optimal Cu^{2+}:Zn^{2+} binding ratio to facilitate development of ZMCs as chemotherapy and radiation sensitizers. Although ZMC1 is not synergistic with chemotherapy and radiation, it is synergistic with a number of other targeted agents.

Introduction

Since the early 1990's, we have known that in addition to its role as a potent tumor suppressor, p53 also plays a role in response to therapy in cancers treated with both cytotoxic chemotherapy and radiation. Both chemotherapy and radiation activate wild-type (WT) p53 resulting in a p53-mediated cell death response that synergizes with the therapy. This is not seen in tumors that are either missense mutant or null for p53 (1, 2). Thus it became known that the p53 status (WT vs. mutant) could serve as a mechanism of sensitivity and resistance to therapies. The mechanism responsible for this activity in large measure is attributed to the DNA damage response pathway signaling on p53 through activation of kinases such as ATM and ATR. These kinases induce posttranslational modifications (PTM) that stabilize the protein and augment recruitment of the transcriptional machinery and in many cases induce an apoptotic program (3). The effect of p53's response to therapy has also served as the rationale for combining drugs that either activate WT p53 (i.e., MDM2 inhibitors, such as Nutlin) or restore WT structure/function to mutant p53 (so-called mutant reactivation) with chemotherapy and radiation to increase efficacy (4–6).

We recently discovered a new class of mutant p53 reactivators called zinc metallochaperones (ZMC) that reactivate specific missense p53 mutants, which share the common defect of impaired zinc binding (7, 8). This is best exemplified by $p53^{R175H}$, the most common missense mutant in cancer, where the substitution of a histidine for an arginine at codon 175 causes steric hindrance close enough in proximity to the zinc coordinating site to weaken the binding affinity for zinc approximately 1,000 fold such that at physiologic concentrations of zinc, the $p53^{R175H}$ is in its apo zinc-free state (9). ZMCs restore WT structure and function using a novel mechanism that involves binding zinc in the extracellular space in a 2:1 molar ratio, which allows the

[1]Department of Molecular Biology, Rutgers University, Piscataway, New Jersey. [2]Program of Surgical Oncology, Rutgers Cancer Institute of New Jersey, Rutgers University, New Brunswick, New Jersey. [3]Department of Surgery, Robert Wood Johnson Medical School, Rutgers University, New Brunswick, New Jersey. [4]Department of Medicinal Chemistry, Rutgers Ernest Mario School of Pharmacy, Rutgers University, Piscataway, New Jersey. [5]Department of Biochemistry and Molecular Biology, SUNY Upstate Medical University, Syracuse, New York. [6]Simmons Comprehensive Cancer Center, University of Texas Southwestern Medical Center, Dallas, Texas. [7]Departments of Pharmacology and Radiation Oncology, University of Texas Southwestern Medical Center, Dallas, Texas. [8]Rutgers Translational Sciences, Department of Chemistry and Chemical Biology, Rutgers University, Piscataway, New Jersey. [9]Z53 Therapeutics, Inc., Holmdel, New Jersey.

Note: Supplementary data for this article are available at Molecular Cancer Therapeutics Online (http://mct.aacrjournals.org/).

S. Zaman and X. Yu contributed equally to this article.

Corresponding Author: Darren R. Carpizo, Rutgers Cancer Institute of New Jersey, 195 Little Albany St., New Brunswick, NJ 08901. Phone: 732-235-7701; Fax: 732-235-8098; E-mail: carpizdr@cinj.rutgers.edu

Mol Cancer Ther 2019;18:1355–65

doi: 10.1158/1535-7163.MCT-18-1080

charge-neutral complex to passively diffuse through the cell membrane as a zinc ionophore, thereby raising intracellular zinc concentrations high enough to overcome the binding affinity defect in the mutant protein (7, 9). With zinc bound in its native ligation site, the protein folds into its WT conformation.

ZMC's must bind zinc with an intermediate affinity that allows them to both bind and donate zinc in the cell (10). We previously measured the Zn^{2+} dissociation constant for the lead compound ZMC1 (K_{Zn}^{ZMC1}) and found this value to be 20–30 nmol/L (9). ZMC1 belongs to the thiosemicarbazone class of metal ion chelators that bind Zn^{2+}, Fe^{2+}, Cu^{2+}, Co^{2+}, and Mn^{2+}. We have recently shown that two other thiosemicarbazones (ZMC2 and ZMC3) bind zinc with similar affinity as ZMC1 (K_{Zn}^{ZMC2} = 27 nmol/L and K_{Zn}^{ZMC3} = 81 nmol/L) and also function as mutant p53 reactivators. However, not all thiosemicarbazones function as ZMCs. Another thiosemicarbazone in clinical development (Triapine, 3-AP) binds zinc too weakly to transport it from the extracellular space into the cell, and is correspondingly nonfunctional ($K_{Zn}^{Triapine}$ > 1 μmol/L; ref. 11).

Another key component of the ZMC1 mechanism relates to p53 PTMs. PTMs are a well-known mechanism for regulating p53 signaling (12, 13). ZMCs generate intracellular reactive oxygen species (ROS), through chelation of redox active metals such as Fe^{2+} and Cu^{2+}. These ROS levels activate a damage response pathway that induces PTMs on the refolded p53 that enhance its function as a transcription factor and drive an apoptotic program (9). In support of this, cellular reducing agents such as N-acetyl-cysteine (NAC) or glutathione (GSH) inhibit ZMC1-induced apoptosis by quenching the ROS signal, leaving ZMC1 capable of inducing a WT conformation change on mutant p53, but unable to transcriptionally activate an apoptotic program (due to lack of PTMs; ref. 9). While these ROS levels play an integral role in the mechanism of ZMC1, they also function as a source of off-target activity that can serve as a source of toxicity.

ZMC1 potently inhibits xenograft tumor growth and improves survival in murine genetically engineered cancer models with zinc-deficient *TP53* mutations through a p53-mediated apoptotic mechanism while having no such effect in tumors that harbor non-zinc–deficient *TP53* mutations (8, 14). Given this unique mechanism, we sought to determine whether the thiosemicarbazone-based ZMCs (i.e., ZMC1) can synergize with cytotoxic chemotherapy or radiation. Using non-thiosemicarbazone–based zinc scaffolds, we sought to determine whether we could potentially separate the p53-refolding activity from the ROS-generating activity by selecting an optimal copper to zinc binding ratio. These new ZMCs would still function to refold mutant p53, but by generating less ROS they might function as chemotherapy and radiation sensitizers. Finally, we sought to use the knowledge of the ZMC mechanism to rationally select targeted agents that might synergize with ZMC therapy.

Materials and Methods

Cell lines, culture conditions, and chemicals

TOV112D, H1299, Detroit 562, H460-shCTL, and H460-shp53 were cultured in DMEM with 10% FBS. TOV112D, H1299, and Detroit 562 were purchased from ATCC. H460-shCTL and H460-shp53 were gifts from Dr. Zhaohui Feng (Rutgers University, New Brunswick, NJ; ref. 15). Cell lines were authenticated by examination of morphology, genotyping by PCR, and growth characteristics. The GSH, cisplatin, irinotecan, 5-Fluorouracil (5-FU), etoposide, adriamycin, β-Lapachone (β-Lap), 6-amino nicotinamide (6-AN), and thionicotinamide (ThioNa) were purchased from Sigma-Aldrich. Nutlin 3a and ABT-199 were purchased from Selleckchem.

Cell growth inhibition assay

Cell growth inhibition assay was performed by MTS, Calcein AM Assay (Trevigen), Vi-CELL Trypan Blue Staining (Beckman Coulter), or Guava ViaCount (Millipore). The procedures are described in Supplementary Data. Statistical significance of the data, obtained from three independent experiments, each with triplicates, was calculated with Student *t* test.

Combination treatment and synergy study

EC_{50} values were calculated from the single-compound treatment assays, measured by MTS assay or Calcein AM assay. Drugs in combination assays were dosed at ratios indicated in each experiment. The combination index (CI) was assessed by the Chou–Talalay method (16, 17) for synergy determination with CalcuSyn Software (Biosoft). CI < 1, synergy; CI = 1, additive; CI > 1, antagonism.

Radiation treatment

The TOV112D cells (100,000 cells/well, in 1 mL culture) were cultured in 12-well plates in duplicate. Cells reached 50%–60% confluence on the second day when cells were treated with indicated treatments and radiation doses. Cells incubated for 3 days, after which cell viability was measured by Vi-CELL cell counter using trypan blue staining.

Immunofluorescent staining

Immunofluorescent staining was performed as described previously (14). The details are in Supplementary Information.

Gene expression (qRT-PCR) and Western blot

The procedures were performed as described previously (14). RNA was extracted from the cells using RNeasy Kit (Qiagen) and the gene expression level was measured by qRT-PCR using TaqMan Gene Expression Assays (Life Technologies/Applied Biosystems). The actin and p53 (DO-1) antibodies were purchased from Santa Cruz Biotechnology. Phospho-p53 (S15), Phospho-p53 (S46), and CDKN1A (p21) antibodies were purchased from Cell Signaling Technology. Acetylated-p53 (K120) antibody was purchased from Millipore.

Transfection of siRNA

The control and p53 siRNA were purchased from Dharmacon. Transfection was performed using RNAiMAX (Invitrogen), following the manufacturer's instructions. The efficiency of the knockdown was measured by Western blot analysis.

Synthesis of ZMC1, 2,2′-((2-Ethoxy-2-oxoethyl)azanediyl) diacetic acid (nitrilotriacetic acid-monoethyl ester), and nitrilotriacetic acid-diethyl ester

The synthesis of ZMC1 (Supplementary Fig. S1), monoethyl ester (MEE), and diethyl ester (DEE) is detailed in Supplementary Data.

K_{Zn} and K_{Cu} measurements

The competition assays used to measure metal dissociation constants are detailed in Supplementary Information.

Oxidative stress detection

ROS signal was measured using CellROX Green Regent (Thermo Fisher Scientific) following the manufacturer's protocol. The p53-null cells were used to minimize any p53 effects.

Colony formation assays

The procedure for long-term viability was performed as described previously (18) and detailed in Supplementary Information

Mouse experiments

Mice are housed and treated according to guidelines and all the mouse experiments are done with the approval of Institutional Animal Care and Use Committee of Rutgers University. The nude mice NCR nu/nu were purchased from Taconic. Xenograft tumor assays were derived from the human tumor cell line, TOV112D (5×10^6 cells/tumor site/mouse). Tumor dimensions were measured every day and the volumes were calculated by length (L) and width (W) by using the formula: volume $= L \times W^2 \times \pi/6$. Tumors (8–12 per group) were allowed to grow to 50 mm^3 prior to daily administration of ZMC1 at 2.5 mg/kg or Nutlin 3a at 5 mg/kg by intraperitoneal administration. ABT-199 (100 mg/mL) was administrated by oral gavage daily.

Statistical analysis

The data were analyzed by Student t test with an overall significance level of $P < 0.05$. *, $P < 0.05$; **, $P < 0.01$; ***, $P < 0.001$.

Results

ZMC1 in combination with cytotoxic chemotherapy or gamma radiation fails to demonstrate synergy

The unique two part mechanism of ZMC1 has been illustrated in which the molecule induces a WT conformation change by restoring zinc binding in the p53R175H (Fig. 1A). As a result of an increase in cellular ROS levels, this newly conformed p53 then undergoes PTMs that enhance its WT transcriptional function and induce an apoptotic program (9).

Given that both cytotoxic chemotherapy and ionizing radiation activate WT p53, we hypothesized that both would synergize with ZMC's. To test this, we treated the human ovarian carcinoma cells TOV112D ($p53^{R175H}$) with ZMC1 combined with cisplatin, irinotecan, 5-FU, etoposide, or adriamycin. We first measured EC_{50}s of each compound alone and then tested the combinatorial treatments. We calculated CI values by CalcuSyn software. Surprisingly, ZMC1 was not synergistic with any of the cytotoxic chemotherapy agents (Fig. 1B; Supplementary Table S1). The combination of ZMC1 and these compounds leads to primarily additive or antagonistic effects. Indeed, when cells were treated with low doses of Adriamycin or Cisplatin concurrently with ZMC1, there was less cell death than in cells treated with ZMC1 alone (Supplementary Fig. S2A and S2B). Moreover, cells were not sensitized to the effects of high dose (1 μmol/L) ZMC1 when treated with ionizing radiation (10 Gy; Fig. 1C).

Synergy between ZMC1 and cytotoxic chemotherapy or radiation is observed when the ROS signal is quenched

Given the role that ROS plays in the ZMC1 mechanism, we hypothesized that the explanation for the lack of synergy between ZMC1 and chemotherapy and radiation could be attributed to this ROS activity. In essence, the signaling events that chemotherapy and radiation would normally induce to activate p53 are already being stimulated by ZMC1. To test this, we attempted to quench the ROS signal generated by ZMC1 using GSH and then combined this with either cytotoxic chemotherapy or radiation. Indeed, when we pretreated TOV112D cells with media containing GSH and then combined this with cisplatin, irinotecan, or etoposide in cell growth inhibition assays, we now observed synergy (Fig. 2A; Supplementary Table S2). Moreover, GSH pretreatment also sensitized ZMC1-treated TOV112D cells to ionizing radiation (Fig. 2B). When we treated another $p53^{R175H}$ cell line (Detroit 562) with ZMC1 and irinotecan, we obtained similar results in that the treatment displayed synergy only in the presence of GSH. The CI value without GSH was 2.32 indicating antagonism, but was 0.87 in combination with 2 mmol/L GSH indicating synergy (Supplementary Fig. S3; Supplementary Table S3).

We have previously demonstrated that ZMC1-induced redox stress functions to induce WT transcriptional function after the mutant p53 protein regains its WT-like structure through PTMs (S15, S46 phosphorylation, and K120 acetylation) that typically drive a p53-mediated apoptotic program (9). This conclusion was made by showing that these PTM's, as well as the WT transcriptional activity of ZMC1 could be silenced by the coadministration of a reducing agent such as NAC (9). In light of this, we found that similar to NAC, these p53 PTMs were inhibited by GSH and consequently WT transcriptional function (p21 expression) was as well (Fig. 2C and D). This signal on p53 could then be restored by treatment with the DNA-damaging agent etoposide in the presence of GSH (Fig. 2C and D). Note the increase in S15 and S46 phosphorylation on p53 with the addition of etoposide to GSH with the concomitant increase in p21 expression. Also note the lack of p21 in the control with etoposide alone (with no ZMC1) indicating that the increase in p21 by etoposide is p53 mediated. We also tested another combination of ZMC1 with irinotecan in the presence of GSH and observed similar results (Supplementary Fig. S4).

To further validate these PTM and p21 expression changes were p53 dependent, we performed similar experiments using the TOV112D cells in the presence of a p53 siRNA, as well as a p53 WT cell line (H460) in the presence and absence of the p53 short hairpin RNA. In the presence of the p53 siRNA, we observed none of the increases in either S15 phosphorylation or p21 levels with any of the treatments in the TOV112D cells (compare Fig. 2C; Supplementary Fig. S5A). We have previously shown in H460 cells that ZMC1 does not activate WT p53 at doses in which it reactivates the $p53^{R175H}$ (14). This is most likely due to the large differences in levels of p53 between the mutant and WT cells. Consistent with those results, we found that ZMC1 did not increase S15 phosphorylation nor p21 levels; however, etoposide alone induced both and this was not modulated by the addition of ZMC1 or GSH (Supplementary Fig. S5B and S5C). This concludes that the ROS signal generated by ZMC1 is enough to stifle synergy with cytotoxic chemotherapy or radiation and that synergy can be produced through a WT p53-mediated activation by quenching the ROS and adding an agent that is known to activate WT p53. Thus the ROS activity of ZMC1 is like a "double edged sword" in that it serves an advantage by making the molecule active as a single agent, but also serves as a disadvantage by inhibiting its ability to synergize with chemotherapy and radiation.

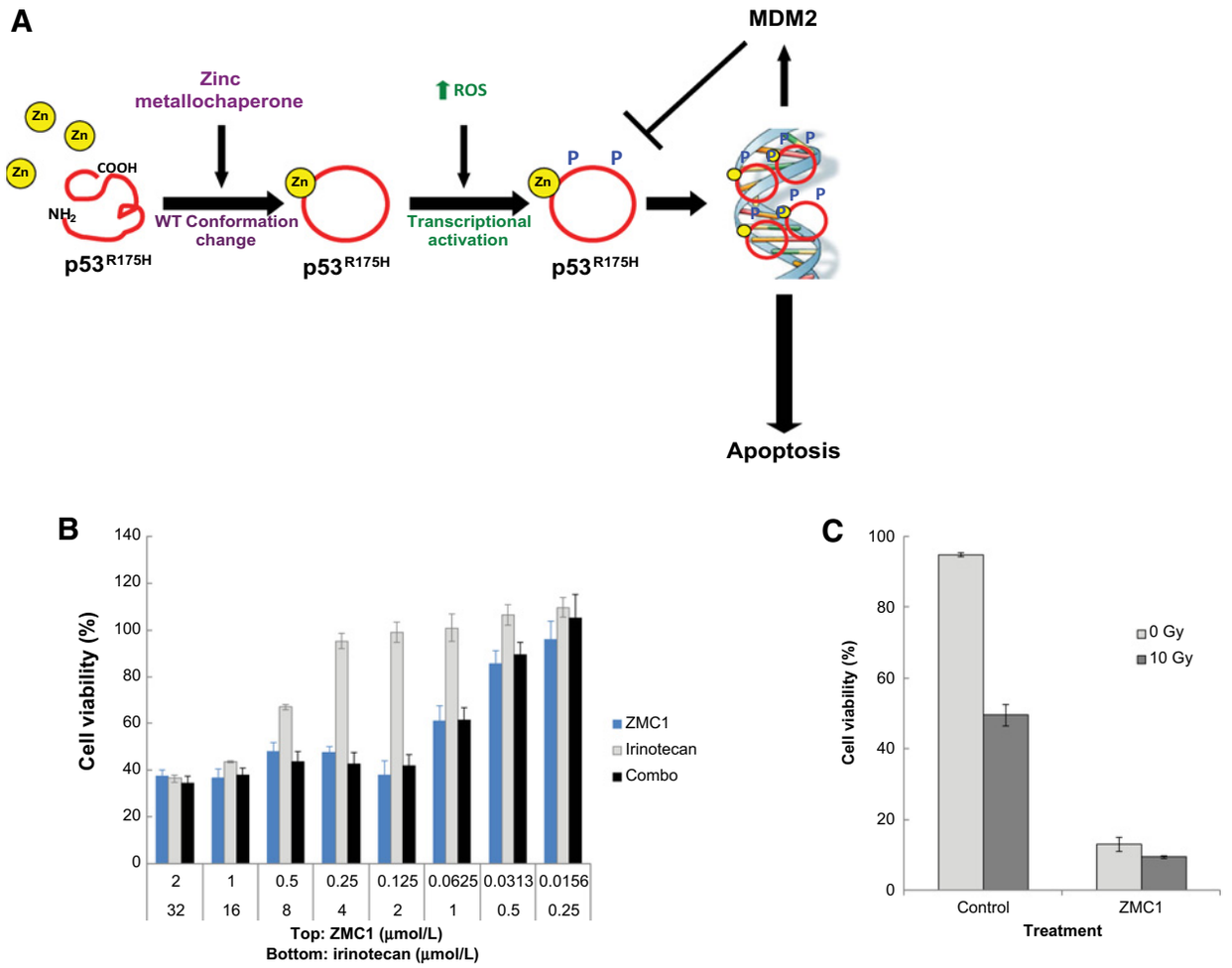

Figure 1.

Combination treatment of ZMC1 and cytotoxic chemotherapy or radiation does not display synergy. **A,** Schematic representation of the mechanisms of ZMC1 reactivating mutant $p53^{R175H}$. **B,** TOV112D (p53R175H) cells were treated with irinotecan, ZMC1, or a combination of both for 72 hours, after which cell viability was measured by MTS assay. **C,** TOV112D cells were treated with gamma irradiation (10 Gy), ZMC1 (2 μmol/L), or a combination of both for 72 hours, after which viability was measured by Vi-CELL trypan blue staining.

Zinc metallochaperones with diminished copper binding synergize with cytotoxic chemotherapy and radiation

If the ROS activity of ZMC1 serves as a disadvantage in combining it with chemotherapy and radiation, then it follows that identifying a ZMC that is capable of inducing a WT conformation change with a marked reduction in ROS activity might possibly synergize with chemotherapy and radiation. This would require an understanding of the source of ROS in ZMC1. Recently ZMC1 (NSC319726) was investigated for its picomolar potency in patient-derived glioblastoma cell lines that was found to be due to increased ROS activity secondary to its copper binding activity (19). Copper, like iron is a redox active transition metal, whereas zinc is not. We measured the Cu^{2+} dissociation constant of ZMC1 (K_{Cu}^{ZMC1}) by means of two independent assays using EGTA or the metal indicator Zincon (20) as competitors for copper binding (Fig. 3A and B; Supplementary Fig. S6). The calculated K_{Cu}^{ZMC1} values of 7.4×10^{-17} mol/L (EGTA competition) and 2.1×10^{-16} mol/L (Zincon competition) reveal that ZMC1 binds Cu^{2+} approximately 10^8-fold more tightly than Zn^{2+} ($K_{Zn}^{ZMC1} = 3 \times 10^{-9}$ mol/L; ref. 9). We hypothesized that identifying a metal-binding scaffold that bound zinc in the range of ZMC1 (to accomplish the conformation change) but bound copper much less avidly might be synergistic with cytotoxic chemotherapy and radiation. We previously demonstrated that nitrilotriacetic acid (NTA) is able to restore a WT-like conformation in mutant p53 as it binds Zn^{2+} with an appropriate affinity ($K_{Zn}^{NTA} = 17$ nmol/L) to function as a zinc metallochaperone (9). However, the NTA·Zn^{2+} complex has an overall anionic character and exhibits poor cell permeability, limiting its utility as a ZMC. To improve the cell permeability of NTA, we replaced the ionizable acids in NTA with nonionizable esters and synthesized the MEE and DEE versions of NTA to be tested in cell culture (Fig. 3C). We anticipated that each esterification step would diminish the molecule's zinc binding affinity by occupying one of the zinc ligand sites. This indeed was evident when we determined the Zn^{2+} dissociation constants to be $K_{Zn}^{NTA\text{-}MEE} = 325$ nmol/L, and $K_{Zn}^{NTA\text{-}DEE} = 850$ nmol/L (Fig. 3D). While the addition of two ester groups to NTA-DEE significantly impaired zinc binding, we

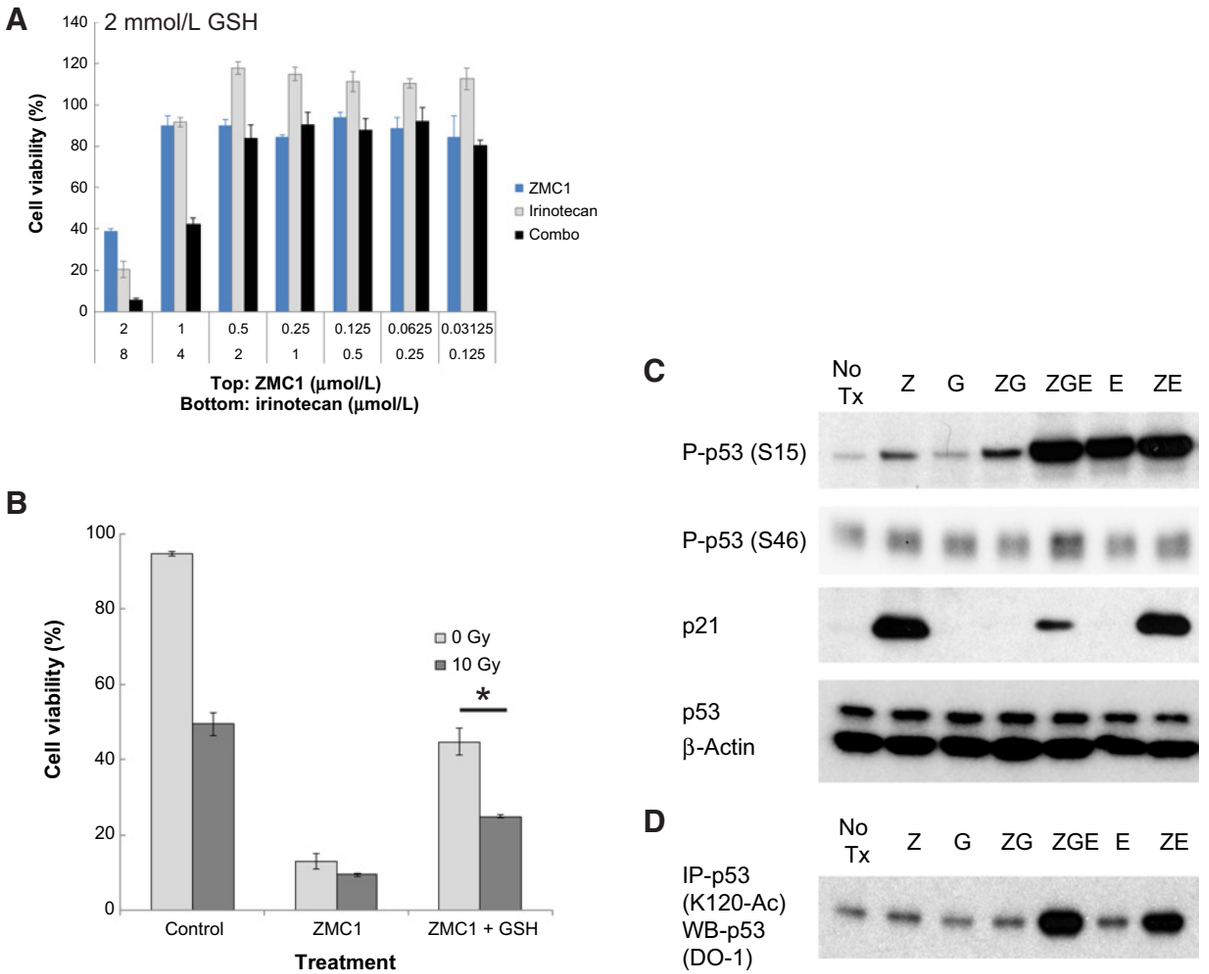

Figure 2.

Combination treatment of ZMC1 and cytotoxic chemotherapy or radiation in the presence of GSH displays increased synergy. **A,** TOV112D cells were treated with irinotecan, ZMC1, or a combination of both for 72 hours in the presence of 2 mmol/L GSH, after which cell viability was measured via MTS assay. **B,** TOV112D cells were treated with gamma irradiation (10 Gy), ZMC1 (2 μmol/L), or a combination of both for 72 hours in the presence of 2 mmol/L GSH, after which viability was measured by Vi-CELL trypan blue staining. *, $P < 0.05$. **C,** Combination treatment of ZMC1 and DNA-damaging reagent (etoposide) in the presence of GSH recovers p53 transcription function as evidenced by p21 expression regulation. TOV112D cells were treated with the indicated compounds for 6 hours followed by analysis of cell lysates by Western blot analysis. The expression of p21 is upregulated by ZMC1 treatment but attenuated with additional GSH. Etoposide treatment restored the p21 expression. Phospho-p53 (S15) and Phospho-p53 (S46) were also detected by Western blot analysis after ZMC1 treatment but attenuated with additional GSH. Etoposide treatment restored the phosphorylation of the p53 protein. β-Actin was used as internal control. **D,** Immunoprecipitation of acetylated p53 (K120). The p53 (K120) acetylation was upregulated by ZMC1 treatment but attenuated with additional GSH. Concurrent etoposide treatment increased the p53 (K120) acetylation. E, etoposide 20 μmol/L; G, GSH 0.5 mmol/L; No Tx, no treatment; Z, ZMC1 1 μmol/L; ZE, ZMC1 and etoposide; ZG, ZMC1 and GSH; ZGE, ZMC1 and GSH and etoposide.

speculated that it might exhibit enhanced biological activity compared with NTA due to increased cellular bioavailability. Once NTA-DEE enters the cell, we reasoned that it could be sequentially hydrolyzed to NTA-MEE and then to NTA by the action of cellular esterases, which are known to act on small-molecule esters (21).

We evaluated the ability of these molecules to function as zinc ionophores and restore WT conformation to the $p53^{R175H}$ by immunocytochemistry using p53 conformation–specific antibodies as previously shown (9, 14). Similar to NTA (5 mmol/L; ref. 9), NTA-MEE (2.5 mmol/L) and NTA-DEE (0.6 mmol/L) induced the WT-like conformation change of mutant $p53^{R175H}$ as evidenced by a significant reduction in fluorescence by the mutant-specific antibody (PAB240) and increase in the WT-specific antibody (PAB1620; Fig. 3E). As expected, the concentrations of NTA-MEE and NTA-DEE required to produce this function were less than that of NTA, consistent with esterification improving cell permeability. However, the fact that all three compounds still required millimolar concentrations to change the p53 immunophenotype suggests that their ionophoric activity remains poor. Using a competition assay with compound C12, a novel chelator that binds Cu^{2+} with much lower affinity than ZMC1 and Zincon ($K_{Cu}^{C12} = 1.3 \times 10^{-11}$ mol/L; Supplementary Fig. S7), we determined the copper dissociation constants of the

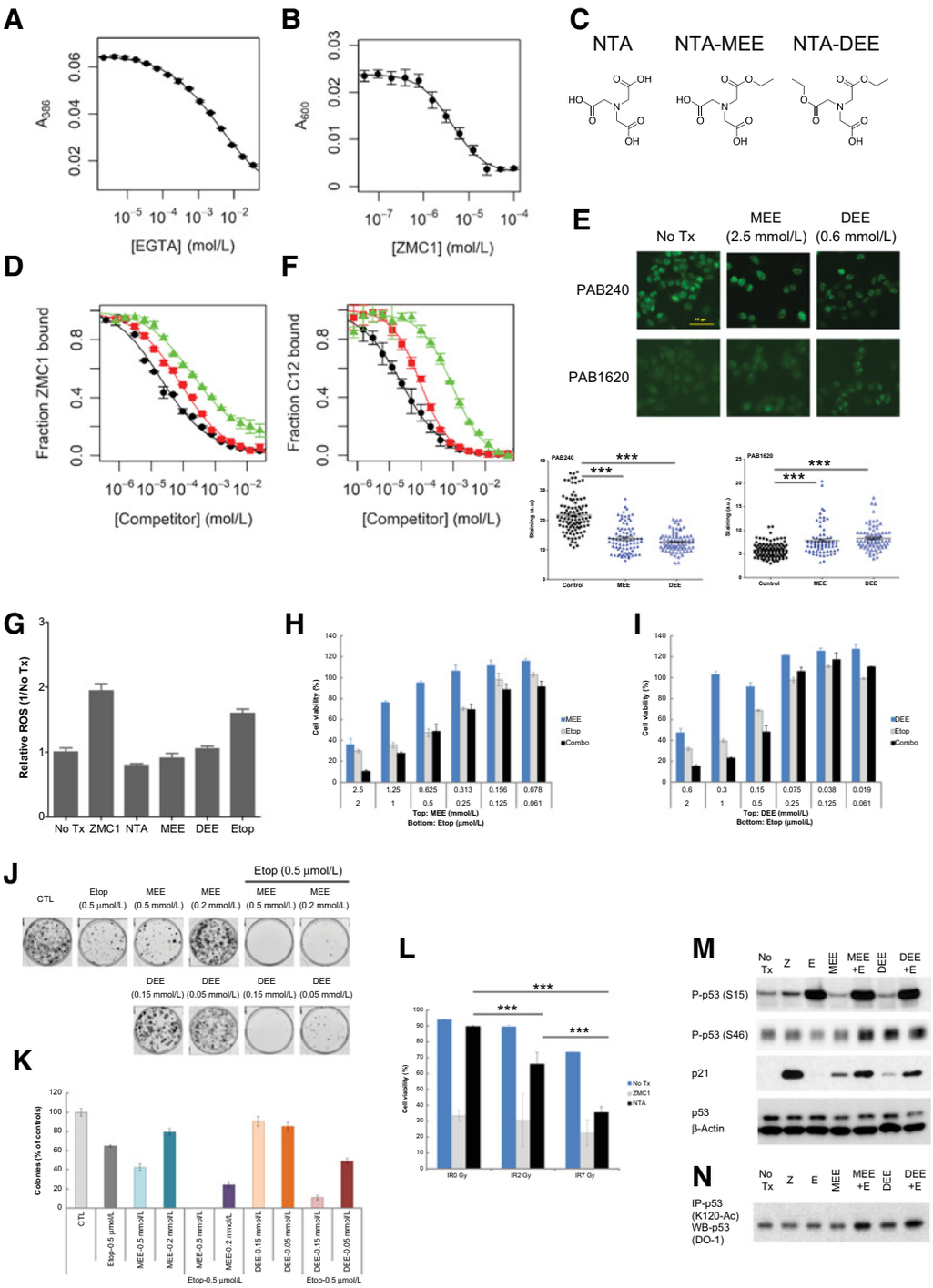

Figure 3.

Combination treatment of p53-reactivating reagent (NTA derivatives) and DNA-damaging reagent (etoposide) recovers p53 transcription. ZMC1 binds Cu^{2+} with K_{Cu}^{ZMC1} values of $(7.4 \pm 0.31) \times 10^{-17}$ mol/L and $(2.0 \pm 0.37) \times 10^{-16}$ mol/L as determined by EGTA competition assays (**A**) and Zincon competition assays (**B**), respectively. **C,** Structures of NTA, NTA-MEE, and NTA-DEE. **D,** NTA (black circles), NTA-MEE (red squares), and NTA-DEE (green triangles) bind to Zn^{2+} with $K_{Zn}^{NTA} = 17$ nmol/L (9), $K_{Zn}^{NTA\text{-}MEE} = (327 \pm 36)$ nmol/L, and $K_{Zn}^{NTA\text{-}DEE} = (850 \pm 350)$ nmol/L as determined by ZMC1 competition. **E,** Immunocytochemistry fluorescence staining (IF) of the p53 protein from TOV112D cells after treatment of MEE (2.5 mmol/L) or DEE (0.6 mmol/L). The antibody PAB1620 recognizes WT conformation of p53. The antibody, PAB240, recognizes mutant conformation of p53. IF quantification was determined using ImageJ. ***, $P < 0.0001$. **F,** NTA (black circles), NTA-MEE (red squares), and NTA-DEE (green triangles) bind to Cu^{2+} with $K_{Cu}^{NTA} = 8.2 \times 10^{-11}$ mol/L (22), $K_{Cu}^{NTA\text{-}MEE} = (2.6 \pm 0.98) \times 10^{-10}$ mol/L, and $K_{Cu}^{NTA\text{-}DEE} = (2.6 \pm 0.92) \times 10^{-9}$ mol/L as determined by C12 competition assay. (*Continued on the following page.*)

NTA compounds to be $K_{Cu}^{NTA\text{-}MEE} = 2.6 \times 10^{-10}$ mol/L and $K_{Cu}^{NTA\text{-}DEE} = 2.6 \times 10^{-9}$ mol/L (Fig. 3F). $K_{Cu}^{NTA\text{-}MEE}$ and $K_{Cu}^{NTA\text{-}DEE}$ are higher than K_{Cu}^{NTA} (8.2×10^{-11} mol/L; ref. 22) by factors of 3.2 and 32, respectively, indicating that esterification of NTA weakens its interaction with Cu^{2+} as well as Zn^{2+}. The most significant result is that, while the NTA compounds bind Zn^{2+} with affinities equal to or only moderately lower than that of ZMC1, the NTA compounds bind Cu^{2+} much more weakly than ZMC1 (10^6- to 10^7-fold). The net result is that the Cu^{2+}:Zn^{2+} selectivity ratio is much higher for ZMC1 (10^8) than it is for NTA and its esters ($10–10^3$).

We then measured the ROS activity of these compounds using the CellROX Green fluorescent agent in p53-null cells treated with various compounds. We used p53-null cells to minimize any changes in ROS due to WT p53 activity. As might be expected from their weakened Cu^{2+} affinities, NTA, NTA-MEE, and NTA-DEE did not induce ROS species like ZMC1 (Fig. 3G). Etoposide induced significant ROS levels similar to ZMC1.

Next, we performed combinatorial experiments with these compounds with etoposide in TOV112D cells and indeed observed synergy (Fig. 3H and I; Supplementary Table S4). We also evaluated the synergy between MEE or DEE and etoposide for a more durable effect using the clonogenic survival assay where cells were exposed to a lower dose of the combination of MEE/DEE plus etoposide. Using a dose of combination that was also relatively insensitive alone, we observed a significant reduction in colonies with the combination (Fig. 3J and K). Moreover, we demonstrate that cells were sensitized to the effects of NTA but not ZMC1 when coadministered with ionizing radiation (Fig. 3L). To investigate the molecular mechanism of the action of this combination treatment, we examined p53 PTMs and p21 levels by Western blot analysis in TOV112D cells. We observed that MEE and DEE alone were capable of inducing some S15 and S46 phosphorylation and K120 acetylation (as well as increase in p21); however, this was diminished in comparison with ZMC1, which is consistent with them producing less ROS than ZMC1 (Fig. 3M and N). When MEE and DEE were combined with etoposide, these PTM's were significantly increased, as well as the levels of p21. Interestingly, etoposide alone did induce an increase in the PTM's we examined, indicating that these PTM's can occur on mutant p53 structure. To provide further evidence that the PTM and p21 responses are p53 dependent, we performed the same experiment in the presence of a p53 siRNA and found no such induction (Supplementary Fig. S8). These results indicate that zinc metallochaperones that are able to reactivate p53 with minimal redox activity can synergize with traditional cytotoxic chemotherapy and ionizing radiation. This represents a new class of ZMCs with the potential to be developed as mutant p53 synergizers with chemotherapy and radiation. Furthermore, we have identified an optimal Cu^{2+}:Zn^{2+} selectivity ratio from which to screen other zinc scaffolds that have better drug-like properties.

ZMC1 in combination with targeted therapeutics

While we have demonstrated that ZMC1 has potent anticancer activity *in vivo* as a single agent (8, 14), we sought to improve this activity through further combinatorial therapy. We took a rational approach to the selection of agents to combine with ZMC1 based upon our knowledge of its unique mechanism of action. We investigated ZMC1 with several other targeted agents that could (i) increase cellular ROS, (ii) interfere with cellular antioxidative regulation, (iii) enhance stability of the activated p53 by blocking Mdm2-p53–negative feedback regulation, or (iv) enhance the apoptotic response (Fig. 4A). β-Lap cycles between its quinone (oxidized) and hydroquinone (reduced) forms, causing both the generation of ROS and a depletion of intracellular reducing agents, namely NADPH within the cell. The reductase, NQO1, is the principal determinant of β-Lap cytotoxicity (23, 24), and ZMC1 treatment upregulates the expression of NQO1 (9). As such, we hypothesized β-Lap could combine synergistically with ZMC1. We chose 6-AN and ThioNa as rational candidates for combination with ZMC1 as they reduce the intracellular NADPH pool (25, 26). ThioNa was previously shown to be synergistic in combination with chemotherapeutic drugs known to induce ROS (26). Using a cell growth inhibition assay, we observed potent synergy when cells were treated concurrently with ZMC1 and β-Lap, 6-AN or ThioNa (Supplementary Fig. S9A–S9C). The CI values were calculated as shown in Supplementary Table S5.

We previously reported that upon undergoing a WT conformation change in the p53R175H by ZMC1, MDM2-mediated negative autoregulation is also restored and the mutant protein levels decrease. This could be abrogated using an MDM2 antagonist (nutlin; ref. 14). If nutlin could stabilize mutant protein levels, there would be more "target" for ZMC1 to act on this wild lead to greater cell kill. In cell culture, we found that the two did indeed synergize, however, at the higher concentrations (EC_{75}, EC_{90}; Supplementary Fig. S9E; Supplementary Table S5). When we examined the effect of the combination of ZMC1 and varying concentrations of nutlin on p53 target gene expression we observed an increase in the expression of *p21*, *PUMA*, *NOXA*, and *MDM2* that was nutlin dose–dependent in comparison with ZMC1 alone (Fig. 4B). Interestingly, the increase in gene

(*Continued.*) **G,** ROS was measured by flow cytometry using CellROX Green Reagent (Invitrogen) in H1299 (p53 null) cells after treatment with the indicated compounds. NTA and its derivatives did not induce ROS. The concentrations of the test are sublethal doses of 0.75 μmol/L. **H,** TOV112D cells were treated with MEE, etoposide, or a combination at the indicated concentrations for 72 hours, followed by cell viability measurement by MTS assay. **I,** TOV112D cells were treated with DEE, etoposide, or a combination at the indicated concentrations for 72 hours, followed by cell viability measurement by MTS assay. **J,** Long-term effect of combination of etoposide and MEE or DEE is evaluated by clonogenic assay. The cells were treated with vehicle control (CTL), etoposide (Etop, 0.5 μmol/L), MEE (0.5 or 0.2 mmol/L), DEE (0.15 or 0.05 mmol/L), or combination. The quantification of colonies is shown in **K**. The *P* value of etoposide versus etoposide + DEE (0.05 mmol/L) is 0.0064. The *P* value of DEE (0.05 mmol/L) versus etoposide + DEE (0.05 mmol/L) is 0.0027. All other etoposide versus combinations and MEE or DEE alone versus combinations have $P < 0.001$. **L,** TOV112D cells are treated with ZMC1 (1 μmol/L) or NTA (5 mmol/L) and 6 hours later, irradiation (0, 2, and 7 Gy) and then incubated for 3 days. The cell viability was measured by Guava ViaCount. Cells treated with NTA are sensitized to ionizing radiation, whereas cells treated with ZMC1 are not. ***, $P < 0.0001$. **M,** Combination treatment of MEE or DEE and DNA-damaging reagent (etoposide) induces p53 transcription function as evidenced by p21 expression regulation, comparable with ZMC1 treatment. TOV112D cells were treated with the indicated compounds for 6 hours followed by analysis of cell lysates by Western blot analysis. The expression of p21 was upregulated by ZMC1, MEE, DEE, or combination with etoposide. Phospho-p53 (S15) and Phospho-p53 (S46) were also detected by Western blot analysis after ZMC1, MEE, DEE, and combination treatment. β-Actin was used as internal control. **N,** Immunoprecipitation of acetyl p53 (K120). The p53 (K120) acetylation was upregulated by MEE, DEE, and combination treatment. DEE 0.6 mmol/L; DEE + E, DEE and etoposide; E, etoposide 20 μmol/L; MEE, 2.5 mmol/L; MEE + E, MEE and etoposide; No Tx, no treatment; Z, ZMC1 1 μmol/L.

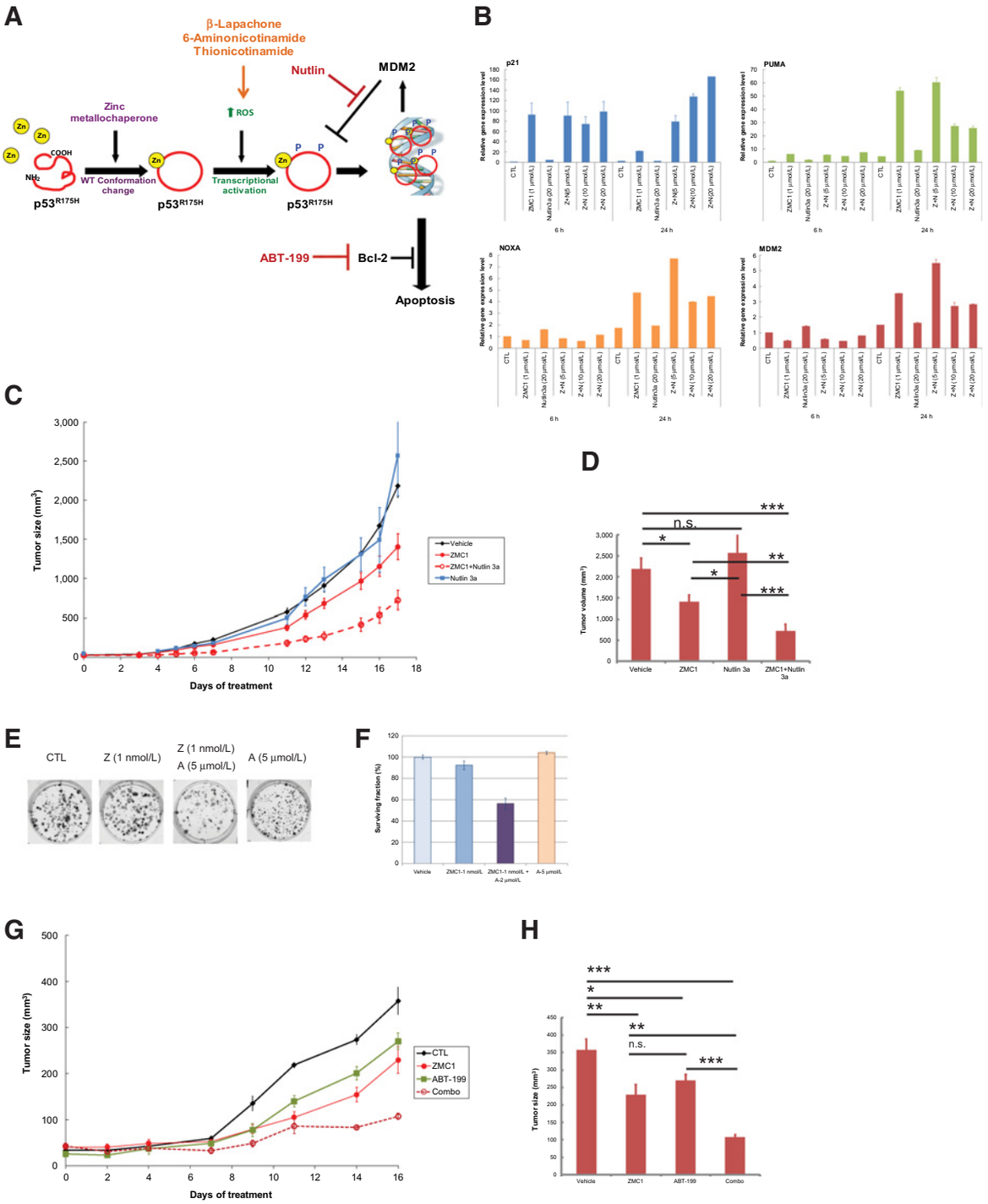

Figure 4.

Combination treatment of ZMC1 and other targeted therapies displays synergy. **A,** Schematic representation of ZMC mechanism and targeted therapeutics. See text for details. **B,** Combination response with ZMC1 and nutlin 3a. The TOV112D cells were treated with ZMC1 (Z, 1 μmol/L), nutlin 3a (N, 5, 10, or 20 μmol/L), or combination of the two compounds. The gene expression levels of the p53 target genes *p21, PUMA, NOXA*, and *MDM2* were measured by qPCR. **C,** *In vivo* efficacy of combination of ZMC1 and nutlin 3a was assessed using xenograft assay of TOV112D cells, as shown the tumor growth curve. The tumor volumes after 17-day treatment are shown in **D**. *, $P < 0.05$; **, $P < 0.01$; ***, $P < 0.001$. **E,** Long-term effect of combination of ZMC1 and ABT-199 is evaluated by clonogenic assay. The cells were treated with vehicle control (CTL), ZMC1 (Z, 1 nmol/L), or ABT-199 (A, 5 μmol/L) and combinations. The quantification of colonies is shown in **F**. **G,** *In vivo* efficacy of combination of ZMC1 and ABT-199 was assessed using xenograft assay of TOV112D cells, as shown in the tumor growth curve. The tumor volumes after 16-day treatment are shown in **H**. *, $P < 0.05$; **, $P < 0.01$; ***, $P < 0.001$. n.s., not significant.

expression was more pronounced at 24 hours as compared with 6 hours. We next evaluated the combination in an *in vivo* tumor growth assay to determine whether this combination would produce greater efficacy than ZMC1 alone. We treated immunodeficient mice bearing TOV112D xenograft tumors with vehicle, ZMC1 alone, nutlin alone, and the combination. While ZMC1 alone administered at 5 mg/kg i.p. is well tolerated and typically inhibits tumor growth by 60% when administered daily in this assay, we had to lower the dose of ZMC1 to 2.5 mg/kg due to toxicity observed with the two agents. ZMC1 at this lower dose could still inhibit tumor growth albeit mildly due this dose reduction (tumor growth inhibition by 36%). As expected there was no inhibition of tumor growth with nutlin alone, whereas we observed significant tumor growth inhibition (67%; $P = 0.0002$) with the combination of ZMC1 and nutlin (Fig. 4C and D).

We previously reported that p53 reactivation by ZMC1 resulted in cell death through a p53-regulated apoptotic pathway (14). Here we chose to test treatment of ZMC1 with ABT-199, an inhibitor of an antiapoptotic protein Bcl-2 (refs. 27, 28; Fig. 4A), and also observed synergy (Supplementary Fig. S9D; Supplementary Table S5). We also evaluated the synergy between ZMC1 and ABT-199 for a more durable effect using the clonogenic assay where cells were exposed to a very low dose of ZMC1 (1 nmol/L), which by itself caused an insignificant decrease in colonies quantified 2 weeks later. Using a dose of ABT-199 that was also relatively insensitive alone, we observed a significant reduction in colonies with the combination (Fig. 4E and F). We next performed Annexin-V staining to determine that the inhibition of cell growth was mediated by apoptosis. We observed an increase in the number of Annexin-V–stained cells with the combination treatment of ZMC1 and ABT-199 (Supplementary Fig. S10). We further evaluated the combination in an *in vivo* tumor growth assay to determine whether this combination would produce greater efficacy than ZMC1 alone. As described before, we treated immunodeficient mice bearing TOV112D xenograft tumors with vehicle, ZMC1 (2.5 mg/kg) alone, ABT-199 (100 mg/kg) alone, and the combination. ZMC1 inhibited tumor growth by 36%, ABT-199 inhibited tumor growth by 25%, whereas we observed significant tumor growth inhibition (70%; $P < 0.001$) with the combination of ZMC1 and ABT-199 (Fig. 4G and H).

Discussion

In this study, we investigated the potential for the development of a variety of combinatorial therapeutic options to enhance the efficacy of a new class of mutant p53 reactivators called zinc metallochaperones. The impetus for this is based on the premise that the effects of cytotoxic chemotherapy and ionizing radiation are potentiated in WT p53 tumors versus mutant ones. It follows from this that the efficacy of a small molecule that restores WT p53 function in a mutant tumor would likely be potentiated by cytotoxic chemotherapy and/or radiation. Our data indicate that a thiosemicarbazone-like ZMC1 while effective as a single agent is not synergistic with either chemotherapy or radiation due to its ROS activity. This is supported by two lines of evidence: (i) synergy with cytotoxic chemotherapy and radiation can be observed when exogenous glutathione is present, indicating that quenching the ROS signal of ZMC1 can permit activation by the addition of DNA damaging agents, and (ii) synergy with cytotoxic chemotherapy and radiation can be observed when using an alternative zinc scaffold that generate less ROS than ZMC1 and is still capable of generating a WT conformation change.

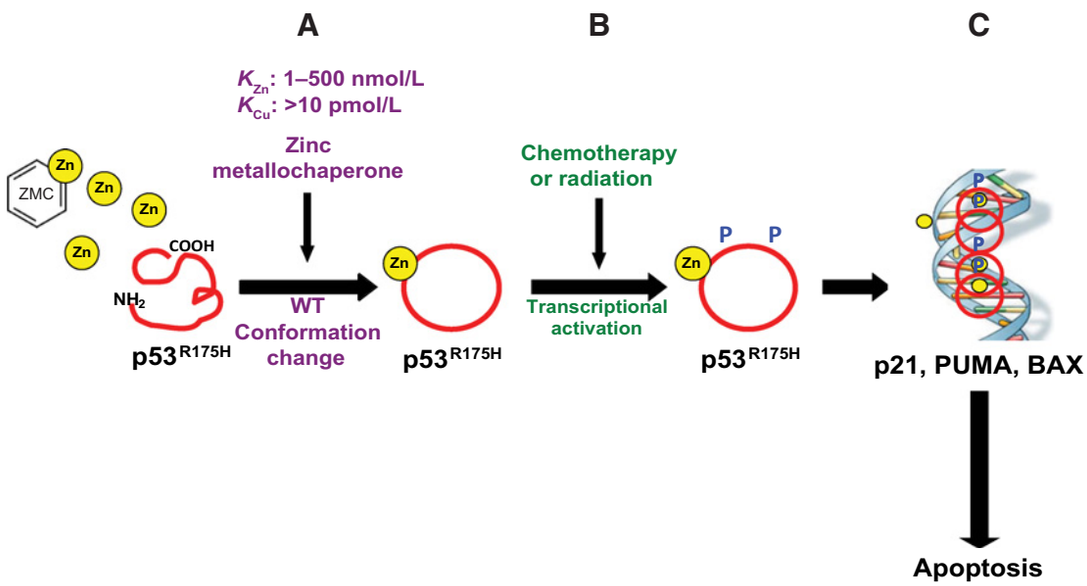

Figure 5.

Schematic representation of the putative zinc metallochaperones with mutant p53 reactivation and diminished copper binding. **A,** The new ZMCs bind zinc in range of 1–500 nmol/L, which allows them to bind zinc tightly enough in the serum for zinc delivery but weak enough to allow them to donate zinc intracellularly to induce a mutant p53 conformation change. Their copper binding would need to be at least weaker than 10 pmol/L, which would lead to a significantly diminished ROS signal. **B,** These compounds can combine with chemotherapy or radiation to promote the newly conformed mutant p53 to undergo PTMs that would activate it to then carry out a p53-mediated apoptotic program (**C**) that would synergize with the chemotherapy and radiation.

The findings that we observed with NTA and the NTA derivatives and their respective copper:zinc binding ratios are important because they provide a new pathway to developing an alternative subclass of ZMC's. This putative ZMC class would be defined by their relative binding affinities for zinc and copper, illustrated in Fig. 5. These new ZMCs would bind zinc in range of 1–500 nmol/L, which allows them to bind zinc tightly enough in the serum for zinc delivery but weak enough to allow them to donate zinc intracellularly to induce a mutant p53 conformation change (Fig. 5A). Their copper binding would need to be at least weaker than 10 pmol/L, which would lead to a significantly diminished ROS signal. When these compounds are combined with chemotherapy or radiation, the newly conformed mutant p53 would undergo PTMs that would activate it to then carry out a p53-mediated apoptotic program that would synergize with the chemotherapy and radiation (Fig. 5B and C). Evidence for this concept has been demonstrated in a preclinical study using a murine breast cancer model (MMTV-neu) in which wt-p53 has been rendered inactive by low expression of HIPK2 resulting in high levels of endogenous metallothioneins that serve to "starve" p53 zinc (29, 30). This model is relatively insensitive to Adriamycin. However, when supplemental zinc was administered by oral administration, the investigators observed a significant reduction in tumor volume and increase in apoptotic activity of the tumors (29).

Our data reveal that the Cu^{2+}:Zn^{2+} binding ratio for NTA and its derivatives is 10–10^3, compared with 10^8 for ZMC1. That NTA, NTA-MEE, and NTA-DEE produce significantly less ROS than ZMC1 allows us to estimate the minimum Cu^{2+} affinity that a metallochaperone must possess to generate ROS in cells. We estimate this value to be $K_{Cu} \leq 10^{-12}$ mol/L. K_{Cu} values greater than this presumably render the compounds unable to compete for Cu^{2+} binding with endogenous sources of the metal. NTA and its derivatives are tool compounds with several shortcomings mostly pertaining to their membrane permeability that we attempted to improve through chemical modification for these proof-of-concept experiments. The identification of a Cu^{2+}:Zn^{2+} binding ratio of 10–10^3 is a major finding of this study. This knowledge will enable us to develop a screen using fluorescent zinc sensors and use copper as a competitive binding partner with which to screen libraries of scaffolds to identify compounds with better pharmacologic properties that have this Cu^{2+}:Zn^{2+} binding ratio.

Although ZMC1 failed to synergize with cytotoxic chemotherapy, we did observe potent synergy with specific-targeted agents on the basis of the understanding of the ZMC mechanism. This is particularly true with agents (e.g., 6-AN and ThioNA) that target metabolic enzymes responsible for replenishing endogenous reducing agents. We have previously shown that ZMC1 depletes cellular glutathione and NADH levels in cells (14), thus we chose 6-AN because it inhibits glucose-6-phosphate dehydrogenase, the enzyme that initiates the pentose phosphate pathway, which is a major source of cellular NADPH. Given the robust synergy of ZMC1 with these agents it is interesting to speculate that ZMC1 may have other metabolic effects on cells that would render them susceptible to ROS-mediated cell death. Recently, the Stockwell group studied the metabolomic effects of NSC319726 (ZMC1) and found that purine deoxyribonucleotides were depleted, whereas pyrimidine deoxyribonucleosides and purine ribonucleosides were not (19). Moreover, Vousden and colleagues recently found that cells that lack WT p53 function are more susceptible to ROS-mediated cell death in conditions of serine starvation (31). Serine is a major precursor for purine nucleotide biosynthesis, and so we speculate that ZMC1's depletion of purine deoxyribonucleotides may be phenocopying the effect of serine starvation.

Our results using the combination of ZMC1 and the BCL2 inhibitor are also interesting as they suggest that perhaps ZMC1 may be functioning in a role of mitochondrial priming by upregulating proapoptotic proteins such as *PUMA*, *BAX*, or *BAK* that can oligomerize at the mitochondrion and lead to mitochondrial outer membrane permeabilization as an explanation for the synergy with the BCL2 antagonist (32).

Our observation that ZMC1 is synergistic both *in vitro* and *in vivo* with an MDM2 inhibitor is also an important result as MDM2 inhibitors are in clinical trials now and there are far greater number of p53-mutant tumors than WT thus mutant p53 reactivating drugs like ZMCs will greatly expand the potential pool of patients that could receive MDM2 inhibitors. Another key finding that supports further experimental use of this combination is the prolongation of expression of several p53 target genes, which in turn resulted in more cell death and tumor growth inhibition after treatment.

Zinc metallochaperones represent a new pathway to reactivate mutant p53 with the potential to treat a very large number of patients. The incidence of cancers that harbor a zinc-deficient p53 mutation is approximately 75,000+ cases in the United States annually, which is a conservative estimate as the number of p53 mutants with a deficiency in zinc binding is growing. Future studies that examine more carefully a range of zinc binding and destabilizing mutants are forthcoming. We expect these studies will reveal a significantly increased therapeutic opportunity for ZMCs by increasing the potential pool of patients whose p53-mutant tumors could be reactivated.

Disclosure of Potential Conflicts of Interest

D.R. Carpizo is founder at Z53 Therapeutics, Inc. No potential conflicts of interest were disclosed by the other authors.

Authors' Contributions

Conception and design: S. Zaman, X. Yu, A.F. Bencivenga, A.R. Blanden, D.A. Boothman, S.D. Kimball, D.R. Carpizo

Development of methodology: S. Zaman, X. Yu, A.R. Blanden, A.J. Blayney, S.N. Loh, D.R. Carpizo

Acquisition of data (provided animals, acquired and managed patients, provided facilities, etc.): S. Zaman, X. Yu, A.F. Bencivenga, A.R. Blanden, Y. Liu, T. Withers, A.J. Blayney, J. Gilleran

Analysis and interpretation of data (e.g., statistical analysis, biostatistics, computational analysis): S. Zaman, X. Yu, A.F. Bencivenga, A.R. Blanden, Y. Liu, B. Na, A.J. Blayney, D.A. Boothman, D.R. Carpizo

Writing, review, and/or revision of the manuscript: S. Zaman, X. Yu, A.F. Bencivenga, A.R. Blanden, J. Gilleran, D.A. Boothman, S.N. Loh, D.R. Carpizo

Administrative, technical, or material support (i.e., reporting or organizing data, constructing databases): X. Yu, J. Gilleran, D.R. Carpizo

Study supervision: X. Yu, D.R. Carpizo

Acknowledgments

This work was supported by grants from the NIH (R01 CA200800 and K08 CA172676), the Breast Cancer Research Foundation (to D.R. Carpizo), and the NIH (F30GM113299, to A.R. Blanden). The authors thank Dr. Zhaohui Feng for providing H460-shCTL and H460-shp53 cell lines.

The costs of publication of this article were defrayed in part by the payment of page charges. This article must therefore be hereby marked *advertisement* in accordance with 18 U.S.C. Section 1734 solely to indicate this fact.

Received September 23, 2018; revised April 8, 2019; accepted June 3, 2019; published first June 13, 2019.

References

1. Lowe SW, Bodis S, McClatchey A, Remington L, Ruley HE, Fisher DE, et al. p53 status and the efficacy of cancer therapy in vivo. Science 1994;266: 807–10.
2. Lowe SW, Ruley HE, Jacks T, Housman DE. p53-dependent apoptosis modulates the cytotoxicity of anticancer agents. Cell 1993;74:957–67.
3. Lakin ND, Jackson SP. Regulation of p53 in response to DNA damage. Oncogene 1999;18:7644–55.
4. Barbieri E, Mehta P, Chen Z, Zhang L, Slack A, Berg S, et al. MDM2 inhibition sensitizes neuroblastoma to chemotherapy-induced apoptotic cell death. Mol Cancer Ther 2006;5:2358–65.
5. Bykov VJ, Zache N, Stridh H, Westman J, Bergman J, Selivanova G, et al. PRIMA-1(MET) synergizes with cisplatin to induce tumor cell apoptosis. Oncogene 2005;24:3484–91.
6. Coll-Mulet L, Iglesias-Serret D, Santidrian AF, Cosialls AM, de Frias M, Castano E, et al. MDM2 antagonists activate p53 and synergize with genotoxic drugs in B-cell chronic lymphocytic leukemia cells. Blood 2006;107:4109–14.
7. Blanden AR, Yu X, Wolfe AJ, Gilleran JA, Augeri DJ, O'Dell RS, et al. Synthetic metallochaperone ZMC1 rescues mutant p53 conformation by transporting zinc into cells as an ionophore. Mol Pharmacol 2015;87: 825–31.
8. Yu X, Kogan S, Chen Y, Tsang AT, Withers T, Lin H, et al. Zinc metallochaperones reactivate mutant p53 using an ON/OFF switch mechanism: a new paradigm in cancer therapeutics. Clin Cancer Res 2018;24:4505–17.
9. Yu X, Blanden AR, Narayanan S, Jayakumar L, Lubin D, Augeri D, et al. Small molecule restoration of wildtype structure and function of mutant p53 using a novel zinc-metallochaperone based mechanism. Oncotarget 2014;5:8879–92.
10. Blanden AR, Yu X, Loh SN, Levine AJ, Carpizo DR. Reactivating mutant p53 using small molecules as zinc metallochaperones: awakening a sleeping giant in cancer. Drug Discov Today 2015;20:1391–7.
11. Yu X, Blanden A, Tsang AT, Zaman S, Liu Y, Gilleran J, et al. Thiosemicarbazones functioning as zinc metallochaperones to reactivate mutant p53. Mol Pharmacol 2017;91:567–75.
12. Meek DW, Anderson CW. Posttranslational modification of p53: cooperative integrators of function. Cold Spring Harbor Perspect Biol 2009;1: a000950.
13. Sykes SM, Mellert HS, Holbert MA, Li K, Marmorstein R, Lane WS, et al. Acetylation of the p53 DNA-binding domain regulates apoptosis induction. Mol Cell 2006;24:841–51.
14. Yu X, Vazquez A, Levine AJ, Carpizo DR. Allele-specific p53 mutant reactivation. Cancer Cell 2012;21:614–25.
15. Zhang C, Lin M, Wu R, Wang X, Yang B, Levine AJ, et al. Parkin, a p53 target gene, mediates the role of p53 in glucose metabolism and the Warburg effect. Proc Natl Acad Sci U S A 2011;108:16259–64.
16. Chou TC. Theoretical basis, experimental design, and computerized simulation of synergism and antagonism in drug combination studies. Pharmacol Rev 2006;58:621–81.
17. Chou TC, Talalay P. Quantitative analysis of dose-effect relationships: the combined effects of multiple drugs or enzyme inhibitors. Adv Enzyme Regul 1984;22:27–55.
18. Franken NA, Rodermond HM, Stap J, Haveman J, van Bree C. Clonogenic assay of cells in vitro. Nat Protoc 2006;1:2315–9.
19. Shimada K, Reznik E, Stokes ME, Krishnamoorthy L, Bos PH, Song Y, et al. Copper-binding small molecule induces oxidative stress and cell-cycle arrest in glioblastoma-patient-derived cells. Cell Chem Biol 2018;25: 585–94.
20. Kocyla A, Pomorski A, Krezel A. Molar absorption coefficients and stability constants of Zincon metal complexes for determination of metal ions and bioinorganic applications. J Inorg Biochem 2017;176:53–65.
21. Kim KS, Kimball SD, Misra RN, Rawlins DB, Hunt JT, Xiao HY, et al. Discovery of aminothiazole inhibitors of cyclin-dependent kinase 2: synthesis, X-ray crystallographic analysis, and biological activities. J Med Chem 2002;45:3905–27.
22. Smith RM, Martell AE. Critical stability constants. Second supplement. Boston, MA: Springer US; 1989.
23. Li LS, Bey EA, Dong Y, Meng J, Patra B, Yan J, et al. Modulating endogenous NQO1 levels identifies key regulatory mechanisms of action of beta-lapachone for pancreatic cancer therapy. Clin Cancer Res 2011;17:275–85.
24. Pink JJ, Planchon SM, Tagliarino C, Varnes ME, Siegel D, Boothman DA. NAD(P)H:Quinone oxidoreductase activity is the principal determinant of beta-lapachone cytotoxicity. J Biol Chem 2000;275:5416–24.
25. Kohler E, Barrach H, Neubert D. Inhibition of NADP dependent oxidoreductases by the 6-aminonicotinamide analogue of NADP. FEBS Lett 1970; 6:225–8.
26. Tedeschi PM, Lin H, Gounder M, Kerrigan JE, Abali EE, Scotto K, et al. Suppression of cytosolic NADPH pool by thionicotinamide increases oxidative stress and synergizes with chemotherapy. Mol Pharmacol 2015;88:720–7.
27. Hockenbery DM, Oltvai ZN, Yin XM, Milliman CL, Korsmeyer SJ. Bcl-2 functions in an antioxidant pathway to prevent apoptosis. Cell 1993;75: 241–51.
28. Souers AJ, Leverson JD, Boghaert ER, Ackler SL, Catron ND, Chen J, et al. ABT-199, a potent and selective BCL-2 inhibitor, achieves antitumor activity while sparing platelets. Nat Med 2013;19:202–8.
29. Margalit O, Simon AJ, Yakubov E, Puca R, Yosepovich A, Avivi C, et al. Zinc supplementation augments in vivo antitumor effect of chemotherapy by restoring p53 function. Int J Cancer 2012;131:E562–8.
30. Puca R, Nardinocchi L, Bossi G, Sacchi A, Rechavi G, Givol D, et al. Restoring wtp53 activity in HIPK2 depleted MCF7 cells by modulating metallothionein and zinc. Exp Cell Res 2009;315:67–75.
31. Maddocks OD, Berkers CR, Mason SM, Zheng L, Blyth K, Gottlieb E, et al. Serine starvation induces stress and p53-dependent metabolic remodelling in cancer cells. Nature 2013;493:542–6.
32. Ni Chonghaile T, Sarosiek KA, Vo TT, Ryan JA, Tammareddi A, Moore Vdel G, et al. Pretreatment mitochondrial priming correlates with clinical response to cytotoxic chemotherapy. Science 2011;334:1129–33.